

Optical properties of Yb films in the far and extreme ultraviolet

Authors: Juan I. Larruquert, José A. Aznárez, José A. Méndez, José Calvo-Angós

Affiliation: Instituto de Física Aplicada-CSIC

C/ Serrano 144

28006-Madrid (Spain)

Phone: 34 91 561 8806

Fax: 34 91 411 7651

Email: larruquert@io.csic.es

Abstract

The optical properties of thin films of Yb in the 53.6-183.6 nm spectral range are presented. Yb films were deposited in ultra high vacuum conditions and their transmittance and reflectance were measured in situ. Transmittance measurements showed that Yb has a certain window of lower absorption between about 54 and 100 nm, which makes Yb an interesting material for filters in this difficult spectral range. The optical constants were obtained out of transmittance measurements and of multi-angle reflectance measurements. These are the first optical measurements on fresh Yb films reported at wavelengths shorter than 107.8 nm. Aging studies were performed both under vacuum and in a desiccator, showing that the optical properties of Yb are strongly modified upon aging.

OCIS codes: 260.7200 Ultraviolet, extreme; 260.7210 Ultraviolet, far; 120.4530

Optical constants; 350.2450 Filters, absorption; 310.6860 Thin films: optical properties

1. INTRODUCTION

The optical constants of many materials have not yet been measured in parts of the far ultraviolet (FUV, 100-200 nm) and extreme ultraviolet (EUV, 10-100 nm). This is the case for most materials of the lanthanide group, because the high reactivity of these materials adds to the general difficulty in performing optical measurements in the EUV-FUV ranges. This paper addresses the optical properties of Yb. Scarce literature is available on the optical properties of Yb in the EUV-FUV. The work of Endriz and Spicer¹ stands out for its completeness and for the careful handling of the samples. They measured the reflectance of Yb and other materials in the 107.8-1240 nm range, from which they obtained the dielectric constant, the absorption, the conductivity, and the loss function. Above 107 nm this work is an optimum reference. Gribovskii and Zimkina² measured the absorption coefficient of Yb and other lanthanides below 17.71 nm. However, between 107.8 nm and 17.71 nm no optical data are available.

The interest in characterizing pure Yb films arises both from a theoretical as well as from a practical point of view. Some calculations are available that predict that Yb may have filtering properties in the FUV-EUV. The semi-empirical approach of Henke et al.³ provides approximate values of optical constants based on the assumption that condensed matter may be modeled as a collection of non-interacting atoms. This assumption is generally acceptable for wavelengths sufficiently far from absorption thresholds and in any case smaller than ~41 nm. Outside the validity domain, the specific chemical state is fundamental and direct experimental measurements must be made. Therefore, the spectral range studied in this paper (53.6-183.6 nm) is not covered by Henke data. In spite of the above, the web page of the Center for X-Ray Optics

(CXRO) at Lawrence Berkeley National Laboratory⁴ provides transmission data (but not the optical constants) of materials, such as Yb, for wavelengths as long as 124 nm, even though no explanation is given as to understand under what assumptions is the model extended to that wavelength. According to those calculations, Yb would be a material with a transmission band approximately in the 50-120 nm range. Such a behavior of Yb would have a practical application for transmission filters able to reject both the EUV below about 50 nm and the wavelengths longer than somewhat above 120 nm. At present only filters of In and Sn are known to have a high transmittance at close regions, and these materials are fragile and hence not very durable. Since no experimental data is available, only by measuring the real transmission of Yb films can the potential of Yb as filters for the EUV be elucidated.

The current paper addresses the optical properties of Yb films in the 53.6-183.6 nm range. The experimental techniques used are described in Section 2. Section 3 shows the transmittance and reflectance measurements performed on freshly prepared Yb films, the optical constants and energy loss function derived from those measurements, and the aging of Yb films both in vacuum and in a desiccator.

2. EXPERIMENTAL TECHNIQUES

Optical measurements were performed in an EUV-FUV reflectometer equipped for in situ ultra high vacuum (UHV) thin film deposition. The reflectometer-deposition system has been described elsewhere^{5,6}. The system basically consists of two interconnected UHV chambers: one for thin film deposition and the other for reflectance measurements. Each chamber was pumped with an ion pump and a titanium sublimation

pump. Both the deposition and the reflectometer chambers were baked out at 470 K. The cryopanel of the Ti sublimation pumps were cooled down with liquid N₂ in order to work under the best possible vacuum of the system. Yb of 99.9% purity from Sigma-Aldrich was sublimated using a Ta boat and the Yb film deposited on room-temperature substrates. The deposition rate ranged between 0.6 and 1.0 nm/s.

Reflectance measurements were performed in situ on samples at room temperature. Films of thicknesses between 39 and 154 nm were prepared. The thickness of films was monitored with a quartz crystal oscillator. These thickness measurements were calibrated through Tolansky interferometry, i.e., through multiple-beam interference fringes in a wedge between two highly reflective surfaces⁷.

The base pressure both in the deposition chamber and in the reflectometer (when isolated from the lamp-monochromator) was $\sim 3 \times 10^{-8}$ Pa after the two chambers were previously baked at 470 K and when using LN₂ to cool the cryopanel. Pressure in the deposition chamber increased during deposition up to $\sim 2 \times 10^{-4}$ Pa, and quickly decreased again once heating was stopped. The sample with the freshly deposited Yb film was quickly transferred under UHV to the reflectometer chamber in about 3 minutes. Yb outgassing during depositions did not decrease upon successive heating and sublimation processes, as one would expect on the basis of the general experience on thermal deposition. The chamber pressure always increased to similar values upon repeated outgassing processes, regardless of the number and extension of these outgassing processes. This was already commented in Ref. 1, and it was explained by the decomposition of hydrides, carbides and nitrides of the sublimating material. The total pressure in the reflectometer during reflectance measurements, i.e. with the

reflectometer connected to the lamp-monochromator, was $\sim 1.5 \times 10^{-7}$ Pa. The main component of the residual atmosphere (measured with a quadrupole mass spectrometer) in the reflectometer when measuring reflectance was the non-oxidizing gas mixture flowing in the discharge lamp, which reaches the UHV reflectometer chamber through a differential pumping arrangement. The gas mixture composition was: 93% He, 3% Ne, 3% Ar, and 1% N₂.

Three different substrates for the Yb films were used. Reflectance measurements were performed on Yb films deposited over 50.8x50.8x3-mm³ float glass substrates that were later polished. Transmittance measurements in the 53.6-104.8 nm range were performed by depositing Yb over a grid previously coated with a C film. Nickel grids were used to support the C film. The grids had square holes with the following nominal characteristics: 5- μ bar, 7.6- μ hole (that corresponds to mesh 2000), 36% open area. The grids were coated with a C film deposited either by arc-evaporation or with an electron beam. Conventional transmission electron microscopy techniques were used to prepare the support C film⁸. C film thickness was of the order of 10 nm. Transmittance measurements at wavelengths of 104.8 nm and above were performed using 12.5x12.5x1-mm³ LiF substrates. In the latter spectral region LiF substrates were used because of the larger transparency of LiF versus a C film over a grid. Either the C film supported on the grid or the LiF substrate were placed in the substrate holder for transmittance measurements. The detector was situated looking at the beam in the position in which the signal measured was at a maximum. Then the sample was alternatively placed in the way of the incoming beam or out of the beam for transmitted and incident intensity measurements, respectively.

3. EXPERIMENTAL RESULTS

Fig. 1.a shows the transmittance of Yb films of different film thicknesses. In order to separate the absorption of Yb from that of the substrate, Fig. 1.a represents the transmittance ratio of a film plus substrate to that of the uncoated substrate. The solid lines in this and other figures are painted to help the eye. The transmittance of the substrates for these particular samples is shown in Fig. 1.b. The transmittance of Yb has a maximum around 58.4 nm. The low absorption band was between ~53.6 nm (it probably goes to somewhat shorter wavelengths, but no shorter wavelength could be measured in our system) and ~100 nm. It is remarkable that the transmission band predicted with calculations performed at CXRO's web page⁴ is close to the experimental measurement, although the transmission peak in the calculations was at 110 nm versus 58.4 nm in our research. The measured transmittance is lower than the calculated one in the coincidence region (53.6-124 nm). As mentioned in the Introduction, the calculations are performed under assumptions that are not clearly stated and they have to be considered only as a very rough guide in the absence of experimental confirmation.

Yb films are not as efficient a potential EUV-FUV filter as it was predicted with the referred calculations. Nevertheless, the transmittance for Yb films may be still adequate for the use of Yb films as filters. Fig. 2 compares the transmission properties of Yb films with those of In and Sn films, which are the available materials for filters in the 50-105 nm range. In and Sn data were taken from Hunter et al.⁹ and Codling et al.¹⁰, respectively. At wavelengths shorter than 53.6 nm, the calculation using CXRO's web page for a 117- nm thick Yb film is also displayed in order to help extrapolate the Yb transmission characteristics. In and Sn main transmittance regions are 75-105 nm and

50-80 nm, respectively. According to our measurements and to the extrapolation, the main transmittance region of Yb roughly combines the transmittance regions of In and Sn, but with a lower rejection above ~100 nm.

The transmittance as a function of thickness was used to obtain the Yb extinction coefficient k , which is the imaginary part of the refractive index ($N=n+ik$; i : imaginary unit), by using:

$$\frac{T_{fs}}{T_s} = \exp\left(-\frac{4\pi kx}{\lambda}\right) \quad (1)$$

where T_s and T_{fs} represent the transmittance of the uncoated substrate and of the substrate coated with an Yb film, respectively. x stands for the film thickness. Yb film samples were prepared in which a new Yb film was deposited over a first Yb film and this process was repeated several times. The transmittance was measured for the uncoated substrate and after every Yb deposition without breaking vacuum. The log plot of the transmittance ratio was fitted versus the Yb film thicknesses. The k values so obtained are plotted in Fig. 3 as a function of wavelength. The current results can be compared with the data of Endriz and Spicer¹ in the coincidence region. Our data are slightly higher than Ref. 1 for most of the wavelengths. Small differences among authors very frequently appear in the current spectral region due to variations in the deposition conditions (material purity, deposition source, deposition rate, base pressure, etc.) and measurements (systematic errors, and also different nature of data: transmittance measurements in the current research versus reflectance measurements plus Kramers-Kronig relations in Ref. 1). In spite of the small differences, the agreement between our results and those of Ref. 1 can be considered as reasonably good

even though in Ref. 1 a lower base pressure and deposition pressure were maintained.

Reflectance measurements as a function of the incidence angle were performed over freshly deposited Yb samples. Fig. 4 shows the reflectance as a function of wavelength for several incidence angles. The reflectance measurements were used to calculate the real part of the refractive index of Yb films, once the imaginary part had been obtained from transmittance measurements.

When the film is not completely opaque to radiation, the film/ substrate interface gives a contribution to the reflectance. In the optical constant calculation of thin films we took into account the interface thin film/ glass substrate. In the calculation we used optical constants of glass substrates that we had previously obtained. The amplitude reflectance of the multilayer vacuum/ thin film/ glass substrate is given by:

$$r^{s,p} = \frac{r_{01}^{s,p} + r_{12}^{s,p} \exp(2i\beta)}{1 + r_{01}^{s,p} r_{12}^{s,p} \exp(2i\beta)} \quad (2)$$

where $r_{ij}^{s,p}$ are the Fresnel reflection coefficients at the interface ij for both parallel (p) or perpendicular (s) electric vector. 0 stands for vacuum, 1 for the thin film, and 2 for the substrate. The propagation function β is given by:

$$\beta = k_0 x (n_1^2 - n_0^2 \sin^2 \theta)^{1/2} \quad (3)$$

where θ is the angle of incidence of the incident beam, x is the film thickness, n_0 is the refractive index of vacuum, n_1 is the complex refractive index of the thin film, and k_0 is the free space wavevector.

Radiation emerging from the monochromator onto the sample is partially polarized. The influence of polarization on reflectance can be described through a single parameter that will be referred to as the degree of polarization p :

$$p = \frac{I_p - I_s}{I_p + I_s} \quad (4)$$

where I_p and I_s indicate the fraction of the incident intensity with the electric vector parallel and perpendicular, respectively, to the plane of incidence. With this notation, the reflectance (ratio of reflected to incident intensity) of the vacuum/ thin film/substrate multilayer for a certain degree of polarization is given by:

$$R = \frac{1+p}{2} R_p + \frac{1-p}{2} R_s \quad (5)$$

where R_p and R_s are the intensity reflectance for p and s polarization, i.e. they equal the square modulus of the amplitude reflectance for parallel and perpendicular incidence, respectively, as they are given in Eq. 2.

The search for the refractive index of films was made by the minimization of the following merit function:

$$s^2 = \sum_{i=1, \dots, m} \left\{ R^{\text{exp}}_{\theta(i)} - R[\theta(i), n, k, p] \right\}^2 \quad (6)$$

where $R^{exp}_{\theta(i)}$ is the reflectance measured at the angle of incidence $\theta(i)$, and $R[\theta(i),n,k,p]$ is the calculated reflectance for the trial value of the refractive index n , using k values obtained from transmittance measurements as known parameters. p for each wavelength in our monochromator had been previously determined. The number of angles of incidence was $m=7$, namely 5° , 25° , 45° , 55° , 65° , 75° , and 80° , all of them in the horizontal plane of incidence of the reflectometer. Regarding surface roughness, a 0.6-nm RMS roughness was measured for the glass substrate by means of atomic force microscopy. We assumed that the surface roughness after depositing Yb was not appreciably larger than for the bare substrate. The reflectance shown in Fig. 4 is small for near-normal incidence, and hence the effect of roughness is to reduce slightly an already small number, which results in a negligible effect over the calculated refractive index. At near-grazing incidence the reflectance values are larger, but the reflectance reduction due to roughness is smaller than at normal incidence in an amount given by an obliquity factor. Based on the above, the surface roughness was neglected in the calculation. The real part of the refractive index calculated with the above model is plotted in Fig. 3, along with data of Ref. 1. The two sets of data show good agreement in the coincidence region for wavelengths up to ~ 130 nm. Above this wavelength our n data are somewhat larger. The optical constants of Yb are also shown in Table 1. The optical constants of the glass substrates, which were used in the refractive index calculation, are shown in Table 2. Both n and k of Yb could have been obtained solely from multi-angle reflectance using the merit function given in Eq. 6, and in fact very similar values were obtained when such a calculation was performed. We proceeded in the two-step method, i.e., we first determined k from transmittance measurements and then calculated n from reflectance measurements, because for low absorbing materials

such as Yb, k values obtained from transmittance measurements are expected to be more accurate.

The above optical constants were used to calculate the loss function $-\text{Im}(1/\epsilon)$ (ϵ : the dielectric function) of Yb films, which is shown in Fig. 5. The main feature of the figure is the peak centered at 124.4 nm (10.0 eV), the two closer wavelengths investigated being 120.0 and 132.0 nm (10.3 and 9.4 eV). A value of ~ 9.6 eV was obtained by Endriz and Spicer¹ from determinations of the dielectric function. Bakulin et al.¹¹ and Colliex et al.¹² performed electron energy loss measurements on Yb films, which were peaked at 9.7 ± 0.1 and 9.7 ± 0.3 eV, respectively. The current determination is compatible with the literature data. A weak bump was found by Bakulin et al.¹¹ and Colliex et al.¹² at ~ 16.5 -18 eV, which was not clearly assessed whether it was a characteristic feature of the metal or it originated in the presence of some Yb oxide along with the metal. In those works, when the loss function was measured over oxidized Yb, a prominent peak appeared centered at ~ 16.7 -17.0 eV. In Fig. 5 there is a weak peak centered at 83.4 nm (14.9 eV). We ignore whether this secondary peak is related with the weak bump of Refs. 11 and 12.

Aging effects in Yb films are very strong due to the reactivity of the material. Fig. 6 summarizes the transmittance degradation of Yb films upon sample storage under UHV, under normal atmosphere, and in a desiccator. The transmittance data labeled as 1, 2, 3 correspond to one sample of Yb over LiF, and 4, 5, 6, 7, 8 correspond to one sample of Yb over a C film supported on a grid; the two samples underwent progressive aging processes. The transmittance decay under UHV was faster in the first hours and the rate decreased over time. But the decay rate did not slow down completely after 5 days of

storage in a desiccator, since after 53 days of storage in a desiccator the further transmittance decay was surprisingly high. Yb films are prone to hidridation under H₂ atmosphere and to oxidation in air¹³. The transmittance decay may then be due to a combination of hidridation, which may be more important under UHV because H₂ is an important residual gas, and of oxidation, which may be more important in air or in the desiccator. The shape of the aged sample transmittance is similar to that of fresh Yb, which means that an unprotected Yb filter would maintain roughly constant the relative transmittance efficiency for the different wavelengths over time.

Aging effects over the film reflectance were also measured. Fig. 7 shows the decay in near-normal reflectance (5°) at wavelengths 132.0-149.2 nm of an Yb film maintained in UHV. Reflectance decayed at a considerable speed in spite of the low pressure. The decay in transmittance was smaller compared to reflectance because transmittance is less dependent on surface effects than reflectance. Fig. 8 shows the effect of 35-day sample storage in a desiccator over its grazing incidence reflectance. The change in reflectance is dramatic. Since the radiation penetration depth at grazing incidence is smaller than at normal incidence, the influence of the modified surface, which has been probably oxidized and/or hydrided, is much stronger.

Summarizing, Yb transmission properties in the FUV-EUV make Yb a promising candidate as a filter with a high transmittance region in the ~50-100 nm, although its high reactivity leaves open the key problem to find a protective material for Yb with adequate transmittance. Protective layers need to be developed in order to prevent the highly reactive Yb from reacting with normal atmosphere or with the residual gases of a vacuum chamber or of a terrestrial orbit for in space astronomy.

CONCLUSIONS

The optical properties of pure Yb films have been measured in the 53.6-183.6 nm. To our knowledge they have been obtained for the first time in the 53.6-107 nm spectral range. The complex refractive index and the loss function were obtained from transmittance measurements and from multi-angle reflectance measurements. Yb films show a low-absorption region in the ~53.6-100 nm, which makes Yb a promising candidate material for EUV filters in a spectral range where In and Sn films are the only available choices and are not very durable.

The high reactivity of Yb results in a fast degradation of transmittance and even more of reflectance. The transmittance decay upon aging is roughly independent of wavelength in the spectral range investigated. The decay of Yb film transmittance leaves open the key problem to find a protective material for Yb with adequate transmittance.

ACKNOWLEDGMENTS

We acknowledge A. Iván Oliva from CINVESTAV, Mérida (Mexico) for AFM measurements on glass substrates. We acknowledge José M. Sánchez Orejuela for his technical assistance. This work was performed under financial support No. ESP2001-4517-PE from the National Programme for Space Research through Spanish Comisión Interministerial de Ciencia y Tecnología.

References

1. J. G. Endriz, W. E. Spicer, "Reflectance studies of Ba, Sr, Eu, and Yb", *Phys. Rev. B* **2**, 1466-1492 (1970).
2. S. A. Gribovskii, T. M. Zimkina, "Absorption coefficients of rare-earth elements of the lanthanum group in the ultrasoft X-ray region", *Opt. Spectrosc.* **35**, 104-105 (1973).
3. B.L. Henke, E.M. Gullikson, and J.C. Davis, "X-ray interactions: photoabsorption, scattering, transmission, and reflection at E=50-30000 eV, Z=1-92", *Atomic Data and Nuclear Data Tables* **54**, 181-342 (1993).
4. http://www-cxro.lbl.gov/optical_constants/
5. J. A. Aznárez, J. I. Larruquert, and J. A. Méndez, "Far-ultraviolet absolute reflectometer for optical constant determination of ultrahigh vacuum prepared thin films", *Rev. Sci. Instrum.* **67**, 497-502 (1996).
6. Juan I. Larruquert, José A. Aznárez, José A. Méndez, "FUV reflectometer for in situ characterization of thin films deposited under UHV" in *Instrumentation for UV/ EUV Astronomy and Solar Missions*, Silvano Fineschi, Clarence M. Korendyke, Oswald H. Siegmund, and Bruce E. Woodgate, eds., *Proc. SPIE* **4139**, 92-101 (2000).
7. S. Tolansky, "Multiple-beam interferometry of surfaces and films", Oxford University Press, London, 1948.
8. P. J. Goodhew, "Specimen preparation in materials science", Vol. I, Part I of the series *Practical methods in Electron Microscopy*, A. M. Glauert ed. (North-Holland Publishing Company, Amsterdam, 1972) pp. 164-167.
9. W. R. Hunter, D. W. Angel, R. Tousey, "Thin films and their uses for the extreme ultraviolet", *Appl. Opt.* **4**, 891-898 (1965).
10. K. Codling, R. P. Madden, W. R. Hunter, D. W. Angel, "Transmittance of tin films in the far ultraviolet", *J. Opt. Soc. Am.* **56**, 189-192 (1966).

11. E. A. Bakulin, L. A. Balabanova, E. V. Stepin, V. V. Shcherbinina, "Characteristic energy losses of electrons in the rare-earth metals", *Soviet Physics-Solid State* **13**, 189-191 (1971)
12. C. Colliex, M. Gasgnier, P. Trebbia, "Analysis of the electron excitation spectra in heavy rare earth metals, hydrides and oxides", *J. Physique* **37**, 397-406 (1976).
13. See for instance: O. Singh, A. E. Curzon, "The effect of oxygen and hydrogen contamination on the electrical resistivity of rare earth metal films", *Thin Solid Films* **44**, 233-240 (1977).

Table 1. Optical constants of Yb films.

wavelength (nm)	n	k
53.6	1.27±0.04	0.040± 0.006
58.4	1.08±0.05	0.035±0.005
67.2	1.08±0.02	0.048±0.004
73.5	0.97±0.02	0.052±0.006
83.4	0.87±0.02	0.106±0.013
87.9	0.86±0.02	0.101±0.009
92.0	0.84±0.02	0.118±0.009
98.6	0.79±0.02	0.143±0.008
104.8	0.76±0.02	0.190±0.005
113.5	0.69±0.02	0.260±0.002
120.0	0.64±0.02	0.343±0.002
124.4	0.63±0.03	0.395±0.003
132.0	0.63±0.03	0.505±0.004
135.7	0.67±0.03	0.548±0.005
141.2	0.70±0.03	0.621±0.005
149.2	0.78±0.03	0.720±0.006
155.7	0.81±0.04	0.71±0.04
174.4	0.88±0.04	0.801±0.007
183.6	0.84±0.04	0.78±0.04

Table 2. The optical constants of glass substrates.

wavelength (nm)	n	k
53.6	0.78	0.39
58.4	0.80	0.47
67.2	0.88	0.60
73.5	0.98	0.67
83.4	1.11	0.70
87.9	1.18	0.75
92.0	1.21	0.77
96.4	1.28	0.79
104.8	1.41	0.81
113.5	1.54	0.78
120.0	1.64	0.73
124.4	1.69	0.71
132.0	1.72	0.68
141.2	1.69	0.60
149.2	1.70	0.51
174.4	1.68	0.39

Figure Captions

Fig. 1.a. The transmittance of Yb films as a function of wavelength for four films of different thicknesses. The transmittance is normalized to the transmittance of the substrate before being coated.

Fig. 1.b. The transmittance of the substrates before being coated with Yb films.

Fig. 2. The transmittance of Yb films of two different thicknesses, normalized to the transmittance of uncoated substrates, compared to that of In (Ref. 9) and Sn films (Ref. 10). The transmittance of Yb calculated with Henke data³ through CXRO's web page⁴ enables extrapolating the current measurements towards shorter wavelengths.

Fig. 3. The optical constants of Yb as a function of wavelength. The data of Ref. 1 is also shown for comparison.

Fig. 4. The reflectance of Yb films versus wavelength at 7 angles of incidence measured from the normal in the horizontal plane of incidence of the reflectometer.

Fig. 5. The loss function of Yb as a function of wavelength.

Fig. 6. The degradation of Yb film transmittance upon aging in UHV, in air and in a desiccator. One film was deposited on a LiF slide and the other one on a C film supported over a grid.

Fig. 7. The degradation of the near-normal reflectance of an Yb film upon aging in UHV.

Fig. 8. The change in near-grazing incidence reflectance of an Yb film upon aging in a desiccator.

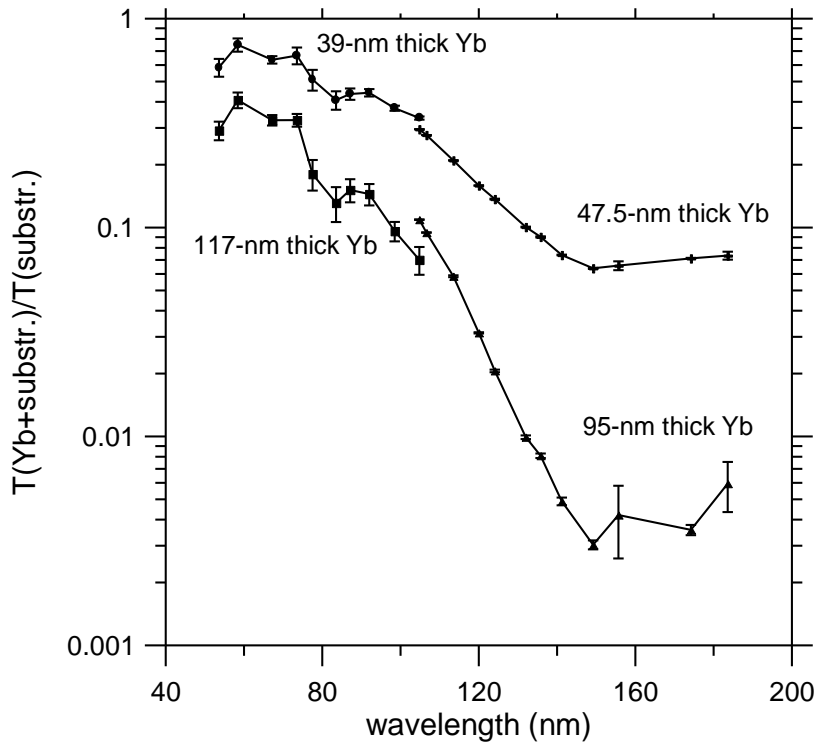


Fig. 1.a
Applied Optics
Juan I. Larruquert

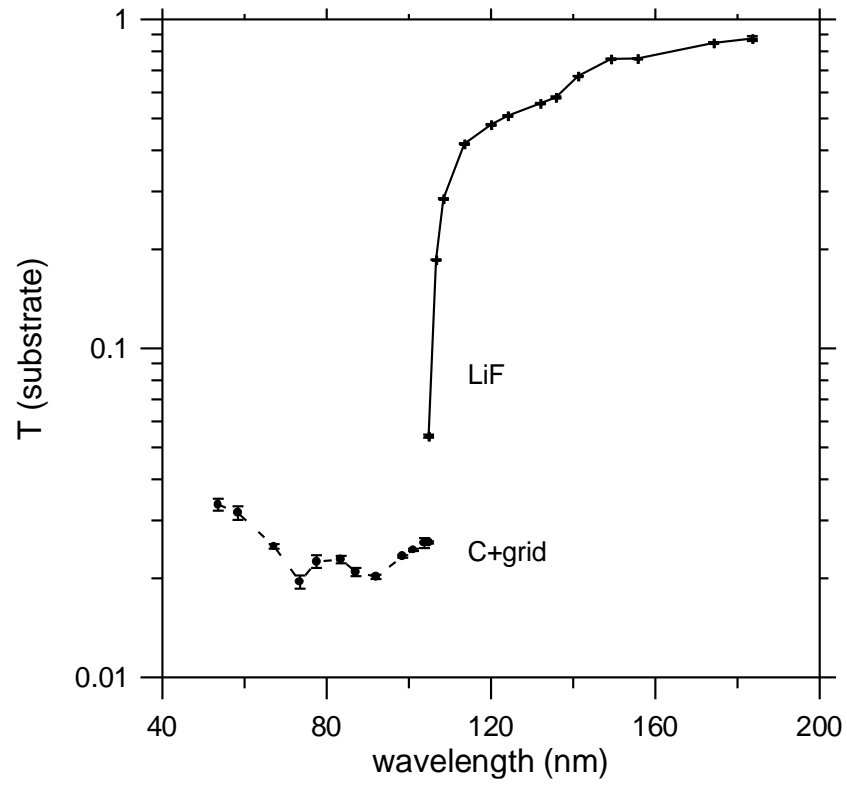


Fig. 1.b
Applied Optics
Juan I. Larruquert

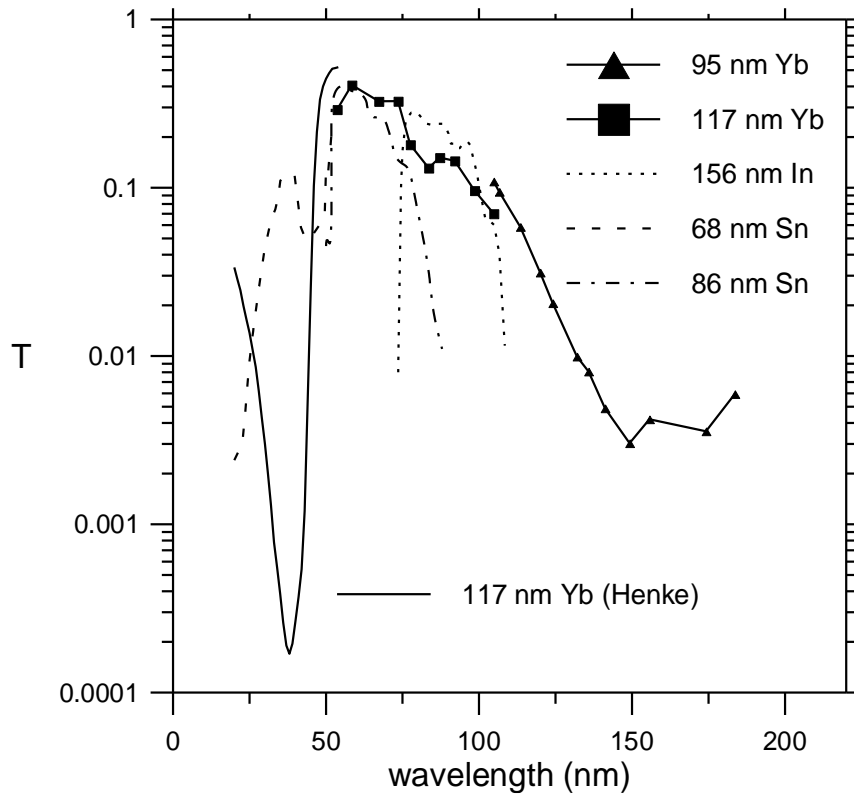


Fig. 2
 Applied Optics
 Juan I. Larruquert

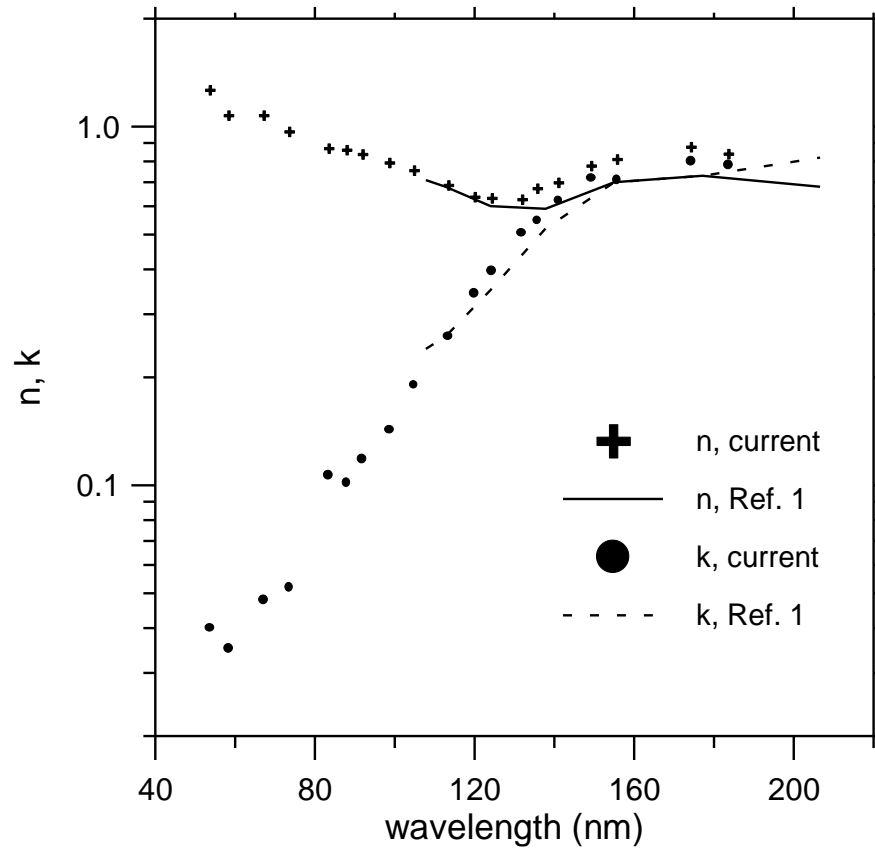


Fig. 3.
 Applied Optics
 Juan I. Larruquert

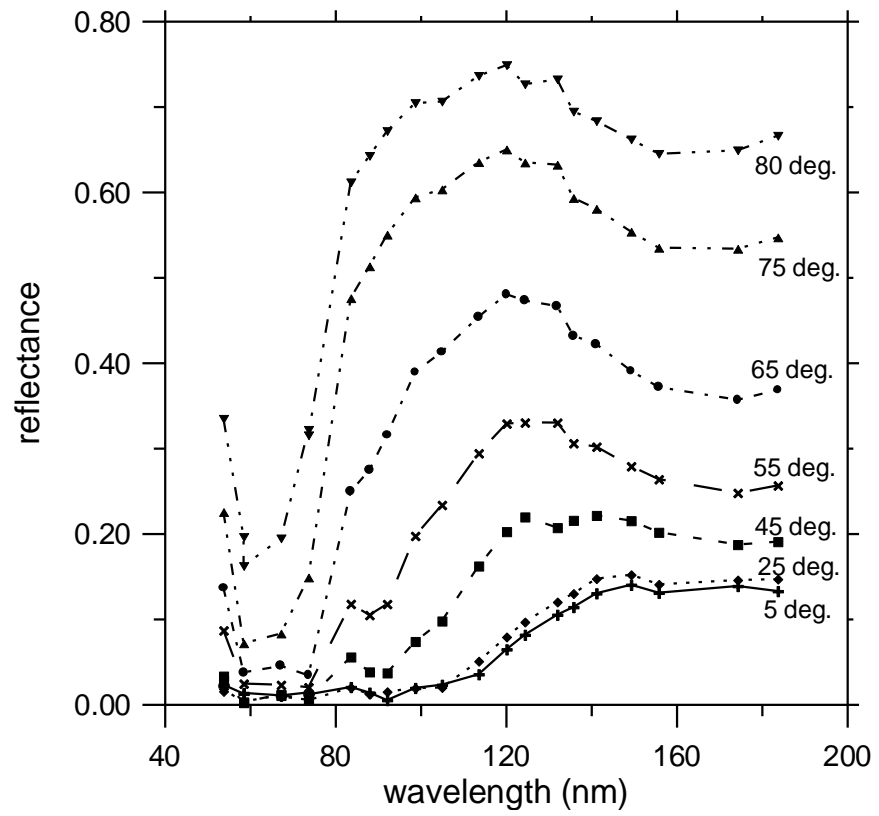


Fig. 4
Applied Optics
Juan I. Larruquert

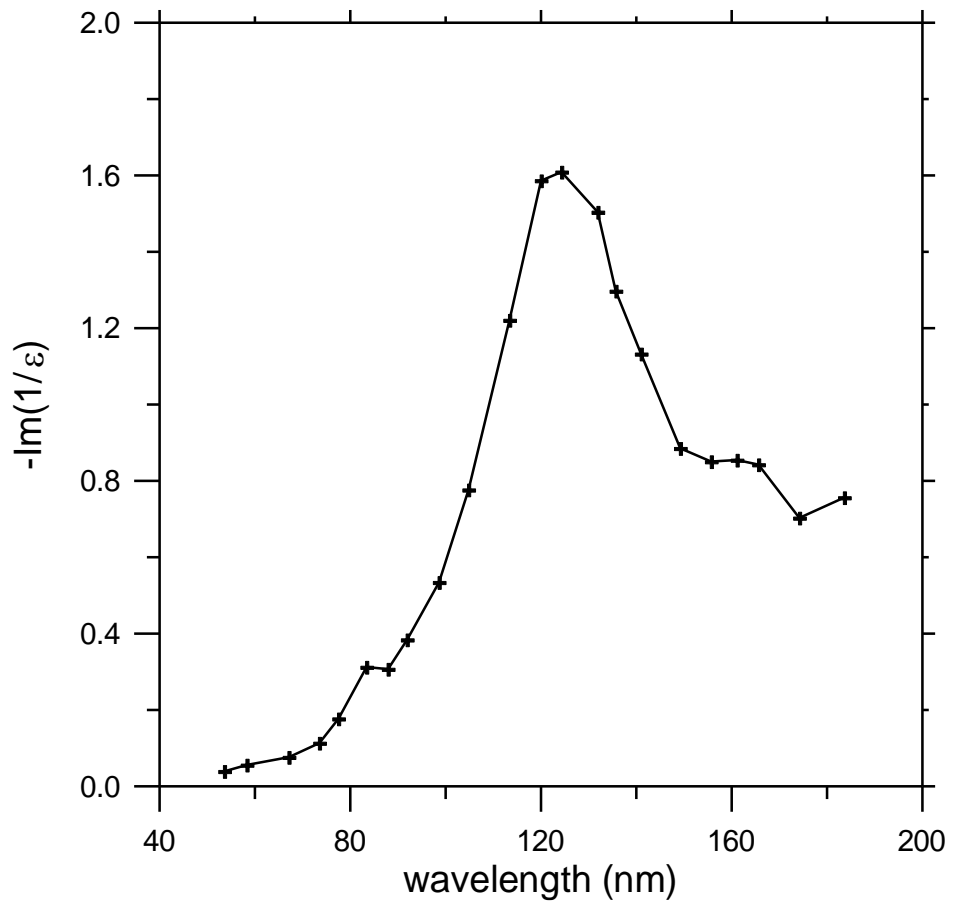


Fig. 5
Applied Optics
Juan I. Larruquert

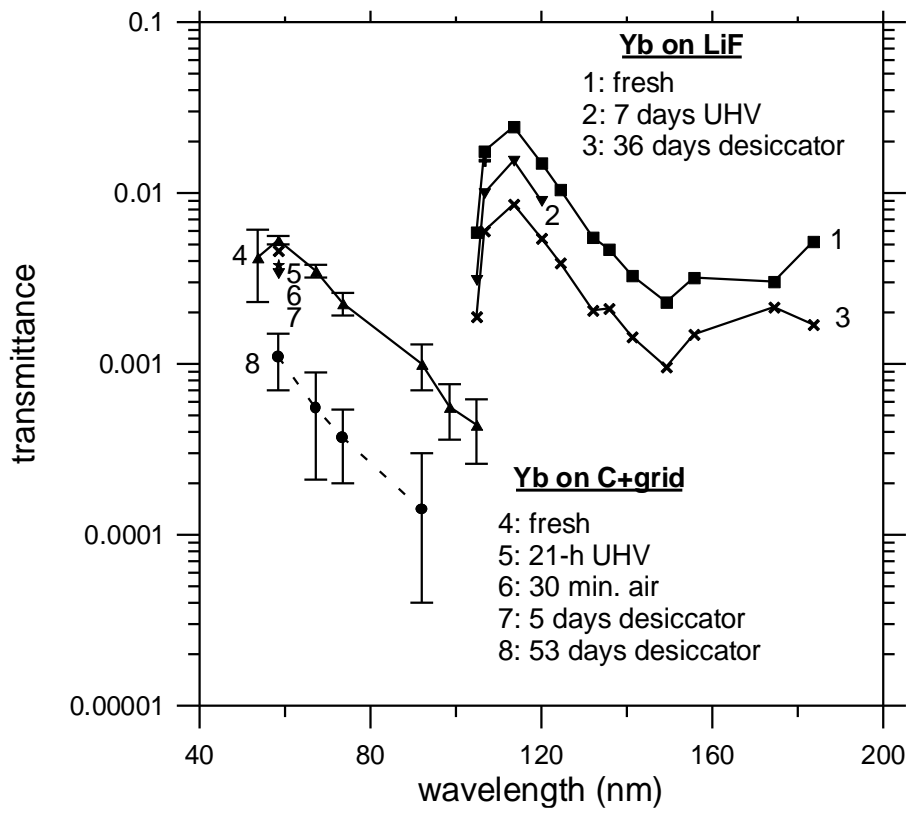


Fig. 6
 Applied Optics
 Juan I. Larruquert

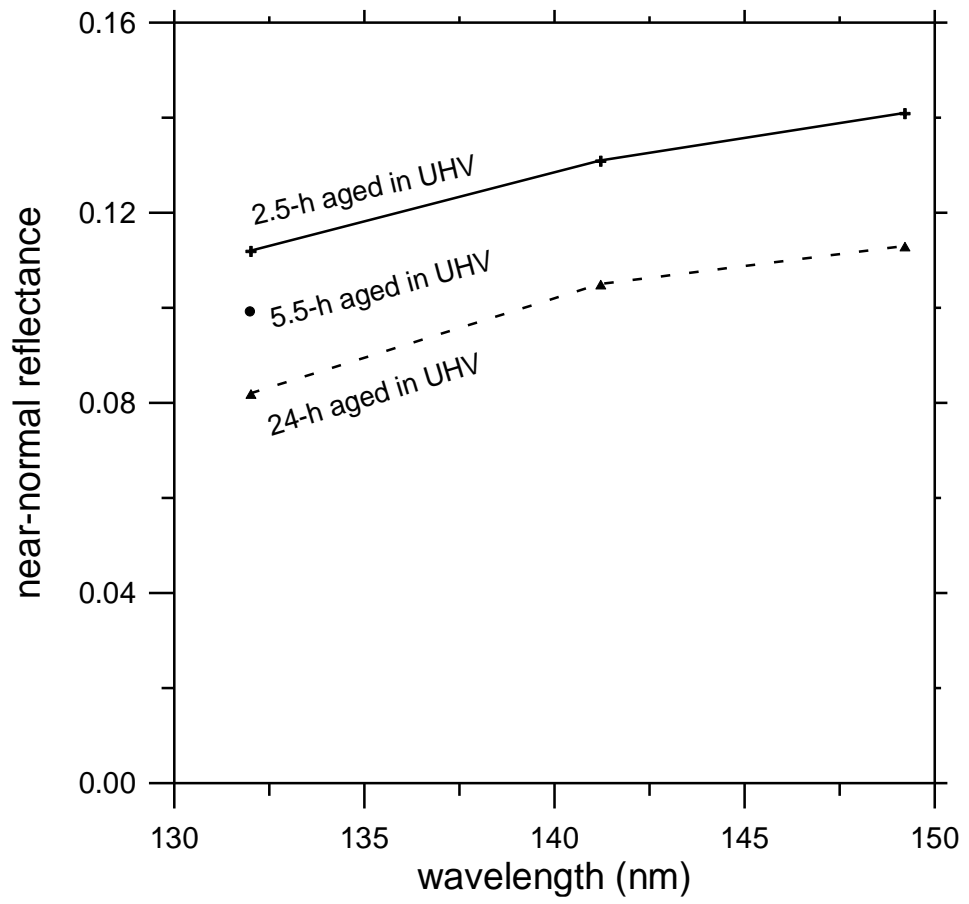


Fig. 7
Applied Optics
Juan I. Larruquert

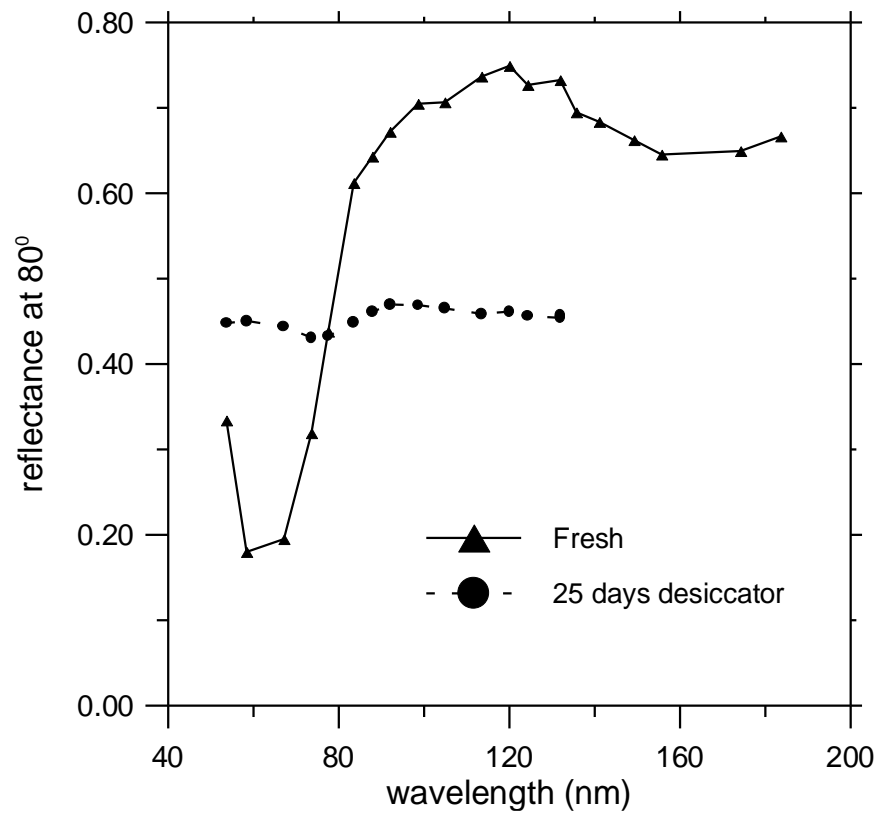


Fig. 8
Applied Optics
Juan I. Larruquert